Molecular Electronics

Deutsche Ausgabe: DOI: 10.1002/ange.201605421
Internationale Ausgabe: DOI: 10.1002/anie.201605421

Covalent Assembly and Characterization of Nonsymmetrical Single-Molecule Nodes

*Christophe Nacci, Andreas Viertel, Stefan Hecht, and Leonhard Grill**

Abstract: *The covalent linking of molecular building blocks on surfaces enables the construction of specific molecular nanostructures of well-defined shape. Molecular nodes linked to various entities play a key role in such networks, but represent a particular challenge because they require a well-defined arrangement of different building blocks. Herein, we describe the construction of a chemically and geometrically well defined covalent architecture made of one central node and three molecular wires arranged in a nonsymmetrical way and thus encoding different conjugation pathways. Very different architectures of either very limited or rather extended size were obtained depending on the building blocks used for the covalent linking process on the Au(111) surface. Electrical measurements were carried out by pulling individual molecular nodes with the tip of a scanning tunneling microscope. The results of this challenging procedure indicate subtle differences if the nodes are contacted at inequivalent termini.*

One of the main motivations for preparing covalently linked molecular nanostructures is their possible use as interconnects in molecular electronics. The idea that individual molecules could exhibit an electronic function goes back to Aviram and Ratner, who proposed single-molecule rectifiers.[1] The concept of monomolecular electronics[2–4] is based on the functionalities of each individual molecule, which interacts specifically with another, in contrast to large ensembles in solution.[5] Key components in molecule-based electronic circuits are molecular nodes: junctions where several molecular chains merge.

Covalent linking of molecular building blocks on atomically defined single-crystal surfaces, so-called on-surface synthesis,[6] is a rapidly growing field.[7–11] Such reactions result in stable oligomers/polymers of well-defined shape and composition, which are given by the chemical structure of the initial building blocks as, for example, realized in a hierarchical linking procedure.[12] Typically, the building blocks can neither be deposited by sublimation nor from solution, owing to thermal decomposition and lack of solubility, respectively. Different covalently linked molecular nanostructures have been obtained on the basis of a variety of chemical reactions and molecular building blocks. They can be classified on one hand as one-dimensional chains, such as polyporphyrins,[13] polyfluorene,[14,15] polyphenylene,[16] graphene nanoribbons,[17,18] and polyethylene strings,[19] which have mainly been studied by scanning tunneling microscopy (STM), but also by more chemical analytical techniques, such as mass spectrometry.[20] On the other hand, two-dimensional networks, either with an approximately rectangular[13,21,22] or with a hexagonal lattice[23–25] can be created if each molecular building block exhibits at least three potential (cross-)linking functionalities.

The synthesis of molecular nodes is very challenging as it requires specific chemical structures, which must be precisely incorporated between the connecting chains. To the best of our knowledge, only one case has been reported thus far, and the synthesis resulted in symmetrical nodes.[17] The ex situ synthesis of functional intramolecular circuits (containing at least one node) is unlikely to be a suitable approach, first because solvent molecules can hardly be avoided, thus not permitting deposition onto a surface under clean conditions, and second because of a lack of compatibility with the future target of a planar assembly of many functional units.

Herein, we present the assembly of three-terminal molecular nodes with various chemical structures of both the node molecule itself and the molecular connectors. Importantly, these nodes connect molecular wires in a nonsymmetrical fashion with chemically different transport channels (in contrast to symmetrical nodes with only one type of channel), a point of key interest for molecular electronics. Although electronic transport in molecular nodes has been described theoretically,[26] no conductance measurements through single nodes exist in which the inequivalent contact geometries, possible with three node connections (and two electrodes), can be controlled.

For the molecular node, we tested hexabenzocoronene-based Br_3HBC (Figure 1a) and hexaphenylbenzene-based Br_3HPB (Figure 1c). These molecules are equipped with Br substituents, which define the linking positions to other molecules[13] and are clearly visible in STM images of intact molecules (Figure 1b,d). The difference between HBC and HPB nodes is that the former are planar aromatic systems, whereas the latter are twisted and exhibit a larger HOMO–LUMO gap as compared to HBC. These trifunctional node molecules were then connected by on-surface synthesis with short oligofluorene monomers (DBTF; Figure 1e) in a non-

[*] Dr. C. Nacci, Prof. Dr. L. Grill
Department of Physical Chemistry
Fritz Haber Institute of the Max Planck Society
Faradayweg 4–6, 14195 Berlin (Germany)
and
Department of Physical Chemistry, University of Graz
Heinrichstrasse 28, 8010 Graz (Austria)
E-mail: leonhard.grill@uni-graz.at
Homepage: http://chemie.uni-graz.at/de/nano
Dr. A. Viertel, Prof. Dr. S. Hecht
Department of Chemistry and IRIS Adlershof
Humboldt-Universität zu Berlin
Brook-Taylor-Strasse 2, 12489 Berlin (Germany)

Supporting information for this article can be found under: http://dx.doi.org/10.1002/anie.201605421.

 © 2016 Wiley-VCH Verlag GmbH & Co. KGaA, Weinheim

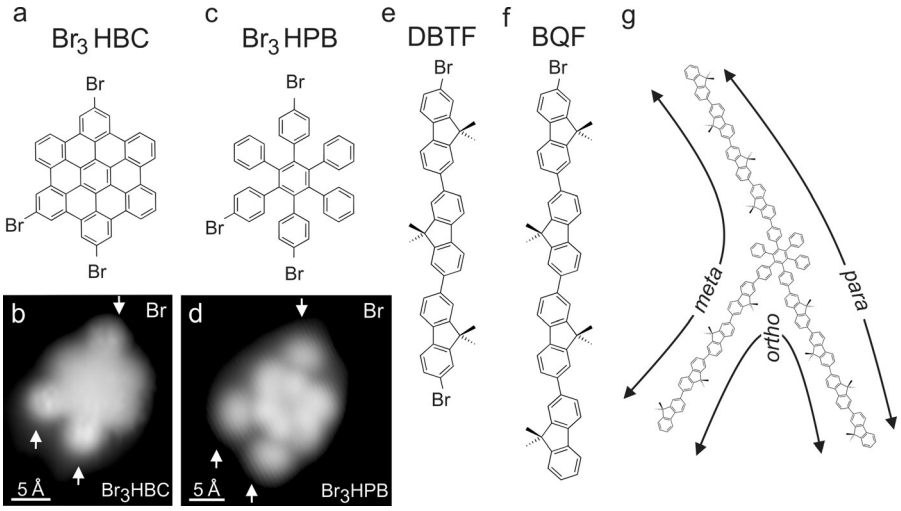

Figure 1. Molecular-node building blocks. a–d) Chemical structures of the hexabenzocoronene (HBC)- and chexaphenylbenzene (HPB)-based molecules studied, each equipped with three Br substituents for on-surface synthesis, and corresponding STM images of single molecules on Au(111). Imaging parameters: b) −50 mV, 100 pA; d) 50 mV, 250 pA. e, f) Chemical structures of dibromoterfluorene (DBTF) and bromoquaterfluorene (BQF). g) Sketch of a molecular node with three linkers attached, resulting in characteristic *para*, *meta*, and *ortho* channels for charge transport.

symmetrical arrangement with *para*, *meta*, or *ortho* π-conjugation paths (Figure 1 g). Experiments were carried out under ultrahigh vacuum with STM at a temperature of 10 K (see the Supporting Information for details).

By depositing Br_3HBC and DBTF molecules onto Au(111) and subsequently heating the sample to 523 K, we succeeded in forming nanostructures from these molecules (Figure 2). New heterostructures were identified, thus proving the successful covalent connection of the different molecular building blocks. However, in comparison with other on-surface synthesis reactions,[12,27] the resulting structures were rather small (see Figure S1 in the Supporting Information for details). Many HBC nodes were connected with only one terfluorene unit (see arrow in Figure 2 a), whereas two-terminal nodes (Figure 2 b–d) were found on a few occasions only (about 5 % of 638 structures), and three-terminal molecular nodes were extremely rare (0.3 %). Besides these few oligomers, individual HBC molecules were present at the surface to a large extent (about 54 %), lacking the three Br substituents. This result indicates that although the dehalogenation process was successful, the linking step was inefficient, presumably owing to limited HBC diffusion as a result of the strong interaction of these molecules with the metal substrate.[28] This interaction became evident in pulling experiments, which turned out to be very inefficient, in contrast to previous studies.[15,29] They failed preferentially at a tip height of about 20 Å (see Figure S2), which precisely matches the distance of the HBC node from the string terminus, and thus the moment at which the node is lifted off the surface. Consequently, the difficulty in the pulling experiments can be ascribed to the rather strong adsorption of HBC on Au(111).[28]

To reduce the interaction of the molecular node with the Au(111) surface, and consequently to enhance the node monomer diffusion for more efficient covalent connection, we employed hexaphenylbenzene (HPB) molecular nodes on Au(111) (Figure 1 c,d). To limit the activation temperature for the covalent coupling and avoid undesired desorption of the molecular nodes, we used iodine substituents instead of bromine on the fluorene molecules (Figure 1 e) owing to their lower activation temperature.[12] After covalent linking (sample heating at 390 K for 5 min), long polymer chains consisting of both HPB and terfluorene units were found on the surface (see Figure S3). The C–C bond-formation process is very efficient as evident from the extended networks, probably as a result of the increased mobility of the molecular HPB nodes (in contrast to HBC nodes; Figure 2). However, these structures exhibit "connectors" with a broad length distribution, that is,

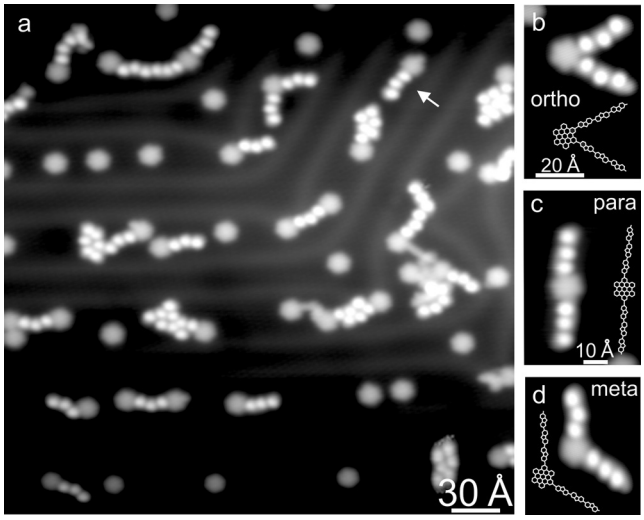

Figure 2. Two-terminal molecular nodes. a) STM topography (343 × 343 Å^2, −0.5 V, 50 pA) of heterostructures comprised of Br_3HBC and DBTF on Au(111) by on-surface synthesis. The arrow indicates a node connected to a single wire. b–d) STM topographies (86 × 86 Å^2, −0.5 V, 50 pA) showing the three different possible channels comprising a HBC node and two terfluorene wires on Au(111): *ortho* (b), *para* (c), and *meta* (d).

long polyfluorene chains, and thus lack the desired control over the final structure.

The growth of well-defined molecular nodes with attached chains therefore requires efficient covalent linking reactions as well as a limited length of the molecular wires. These conditions, somewhat contradictory, led us to a new molecular building block: bromoquaterfluorene (BQF; Figure 1 f), which exhibits only one terminal Br substituent, thus guar-

 © 2016 Wiley-VCH Verlag GmbH & Co. KGaA, Weinheim

anteeing that the on-surface reaction is limited to the addition of one quaterfluorene (QF) unit only and prohibiting the formation of extended polyfluorene structures.

After the deposition of trifunctional Br_3HPB (Figure 1c,d) and BQF (Figure 1f) onto Au(111) and subsequent sample heating, no extended networks were identified (as with diiodoterfluorene molecules), but rather small structures of defined length, according to the presence of only one halogen substituent, that is, one potential reactive site, in each quaterfluorene molecule. Three-terminal molecular nodes—consisting of the node building block and precisely three short molecular wires, one at each linking site—were clearly visible as individual units or in weakly coupled clusters (Figure 3b).

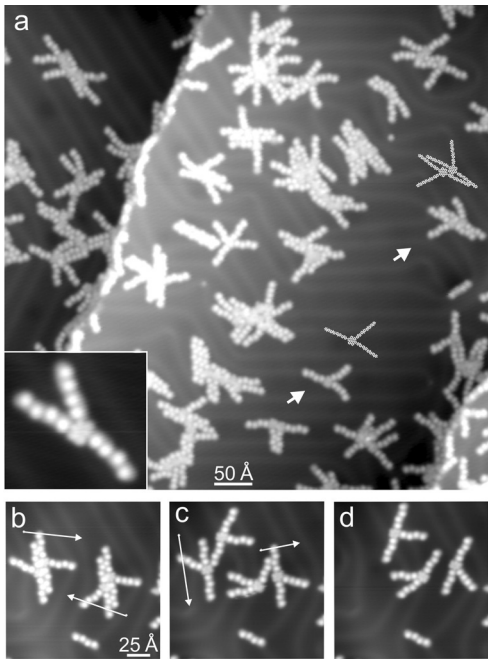

Figure 3. Three-terminal molecular nodes. a) Constant-current STM image (686×686 Å^2, 1 V, 50 pA) taken after dehalogenating the species on the surface. Individual molecular nodes and node clusters were also identified (see arrows and the chemical structures). Inset: STM image (1 V, 50 pA) of an individual three-terminal molecular node. b–d) Untangling of molecular-node clusters by STM-based lateral manipulation. Sequence of constant-current STM images (192×189 Å^2, 1 V, 50 pA) showing molecular nodes untied by constant-current lateral manipulation (set point: 25 mV, 20 nA). The arrows represent the direction along which the manipulation took place. The molecular node manipulated in (c; left) is missing in (d), probably because it was picked up by the STM tip.

Other structures were also present on the surface (see Figure S4), but a substantial fraction of the molecular structures (29% of 604) were in the predefined three-terminal-node configuration (Figure 1g), in agreement with a simple statistical model (see Figure S6). These nodes were highly defined in terms of composition, dimensions, and symmetry. In contrast to the covalent HPB–fluorene bonds, three-terminal molecular nodes in clusters were held together by weak interactions and could be separated readily by STM manipulation (Figure 3b–d). The weak interaction between the molecular structures is evident from the rather gentle manipulation conditions, with a tunneling resistance of about 1.25 MΩ (20 nA at a bias voltage of 25 mV) being sufficient to overcome the potential-energy barrier for separation. These manipulation experiments[30] resulted in individual node structures (inset of Figure 3a), which is not only important for the unambiguous identification of the cluster structures, but also for pulling experiments[15] with single-node structures. In a few instances, we observed the formation of molecular nodes with more than three quaterfluorene legs/arms attached (as in the center of Figure 3a). Owing to the very low abundance (ca. 2%) of these species on the surface (see the Supporting Information for details), no structural insight into the nature of the attachment and the underlying chemical mechanism could be obtained thus far.

The central question in conductance experiments by pulling with the STM tip was whether any difference between the *para*, *meta*, and *ortho* transport channels (Figure 1g) could be distinguished in single molecular nodes. Accordingly, three configurations can be defined in a pulling geometry (Figure 4a–c) with two superimposed tunneling transport

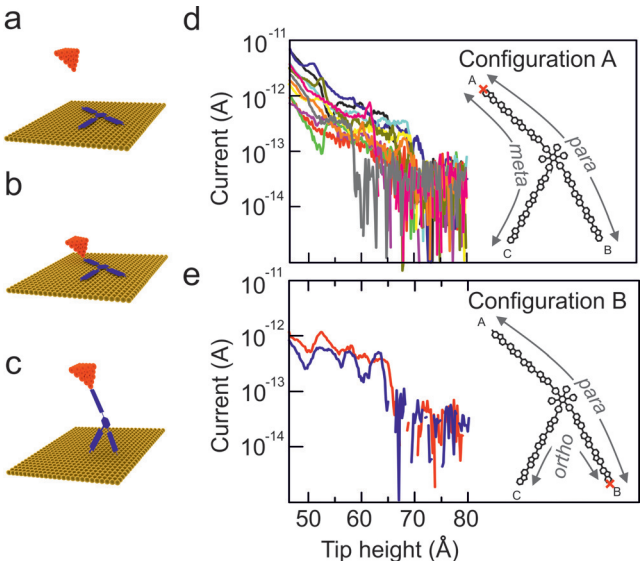

Figure 4. Single-molecular-node conductance measurements. a–c) Schematic illustration of the STM pulling process: a) Vertical approach of the STM tip towards the surface; b) contact between the STM tip and the molecular-wire terminus; c) tip retraction: the wire is pulled off the surface. d, e) $I(z)$ pulling curves related to configurations A and B. The current is plotted at tip heights above 45 Å; from geometric considerations of the QF–HPB length, only above a tip height of 45 Å is it clear that the molecular node itself is lifted from the surface and thus contributes to the current in the junction.

channels: configuration A with charge transport along *para* and *meta* channels (Figure 4d), configuration B with charge transport along *para* and *ortho* channels (Figure 4e), and *ortho* and *meta* channels in the case of configuration C (not shown). During the pulling process, we chose an individual defect-free molecular node in the STM image and then selectively contacted the STM tip with one of the three, inequivalent, oligofluorene strands. The current dropped

© 2016 Wiley-VCH Verlag GmbH & Co. KGaA, Weinheim

when the contact between the tip and the molecular structure was lost, typically at a vertical tip height of around 70 Å (Figure 4 d,e), which corresponds approximately to the maximum length of the node structure (i.e. along the *para* configuration) in the junction. Hence, the current drop is a signature for complete removal of the molecule from the surface.

Although the node component (HPB) adsorbs less strongly than the HBC molecule, the total molecule–surface interaction remained strong enough to render the pulling experiments very difficult with a success rate (over all configurations) of about only 3% (over 844 attempts). Interestingly, the success rates differed strongly, with the best efficiency for configuration A (about 10%) and a much reduced yield for configuration B (about 1%), whereas configuration C could not be lifted successfully and measured at all. We attribute these differences, which can not be caused by the HPB node, primarily to the lateral bending angle of the two quaterfluorene linkers that remain in contact with the surface when the third is pulled. For example, in the simple case of only two linkers in a *para* configuration (attached at opposite sites to the node), this lateral bending angle with respect to the node would be zero (note that bending *off* the surface of course takes place). When going now from configuration A to C, the bending angles of the surface-attached linkers increase, which raises the energy barrier for the process, thus rendering pulling more difficult. Considering the prerequisites for a pulling experiment, that is, to find a molecular node structure in a defect-free area and to disentangle it from other node structures by lateral manipulation (Figure 3 b–d), a successful pulling experiment is an extremely challenging and therefore very rare event.

Conductance $I(z)$ curves were measured for configurations A and B (all successful events are plotted in Figure 4 d,e), and an approximately exponential decay behavior was found for both. Hence, the conductance G of individual configurations was determined on the basis of the inverse decay length β by $G = G_o e^{-\beta z}$ (G_o is the contact conductance and z the electrode distance).[15,29] The obtained $I(z)$ curves are superimposed by oscillations that are probably caused by the mechanical properties of the molecular structure, the intramolecular degrees of freedom, during the pulling process, as found in previous studies.[15,31] These intramolecular rotary and bending motions can also affect the conjugation in the molecules and consequently the charge transport through them as visible in the current curves.

These electrical measurements through individual molecular nodes with full control over the contacting geometry (configuration A or B) proved very difficult, and therefore, despite substantial experimental effort in time-consuming measurements, only very few conductance curves $I(z)$ could be obtained. On the basis of the acquired data (Figure 4 d,e), it appears that the current curves point to a different behavior in the two configurations, whereby configuration B seems to exhibit better conductance (i.e. smaller decay) than configuration A. This observation was quantified by a statistical analysis, from which we extracted very small β values of $\beta_A = (0.053 \pm 0.008)$ Å^{-1} and $\beta_B = (0.020 \pm 0.010)$ Å^{-1} (bias voltages between −1.8 and −1.9 V), which are clearly smaller than for single polyfluorene wires[15]—probably because here two wires are arranged in parallel. Hence, more efficient charge transport seems to be present in configuration B, which combines both π-conjugated *ortho* and *para* channels, as compared to configuration A, which involves a π-conjugated *para* channel in combination with a cross-conjugated *meta* channel. Owing to the limited number of successful pulling experiments, our results, however, should be regarded with some caution, and future measurements, involving for example a flat geometry and multiple tips, should be carried out to validate this finding.

In conclusion, we have shown how molecular three-terminal wire–node architectures—highly defined in terms of dimensions, composition, symmetry, and geometrical arrangement—can be formed. Rather small changes in the chemical structures of the compounds involved had a profound effect on the products of the on-surface synthesis, owing to characteristic diffusion properties and reactivities. Different electrical currents were measured through single molecular nodes, depending on the precise location of the electrode contacts with respect to the three connectors, however, in only very few successful cases. First indications of different transport behavior depending on the contributing conjugation pathways through the node molecule have been revealed.

Acknowledgements

Important discussions with Christian Joachim and Francisco Ample are gratefully acknowledged. We thank the European Union for financial support through the AtMol project.

Keywords: conjugation · molecular electronics · molecular nodes · scanning probe microscopy · single-molecule manipulation

How to cite: *Angew. Chem. Int. Ed.* **2016**, *55*, 13724–13728
Angew. Chem. **2016**, *128*, 13928–13932

[1] A. Aviram, M. Ratner, *Chem. Phys. Lett.* **1974**, *29*, 277.
[2] J. M. Tour, *Acc. Chem. Res.* **2000**, *33*, 791.
[3] C. Joachim, J. K. Gimzewski, A. Aviram, *Nature* **2000**, *408*, 541.
[4] J. R. Heath, M. A. Ratner, *Phys. Today* **2003**, *56*, 43.
[5] A. P. de Silva, S. Uchiyama, *Nat. Nanotechnol.* **2007**, *2*, 399.
[6] D. F. Perepichka, F. Rosei, *Science* **2009**, *323*, 216.
[7] A. Gourdon, *Angew. Chem. Int. Ed.* **2008**, *47*, 6950; *Angew. Chem.* **2008**, *120*, 7056.
[8] L. Bartels, *Nat. Chem.* **2010**, *2*, 87.
[9] M. Lackinger, W. M. Heckl, *J. Phys. D* **2011**, *44*, 464011.
[10] J. Méndez, M. F. López, J. A. Martín-Gago, *Chem. Sov. Rev.* **2011**, *40*, 4578.
[11] Q. Fan, C. Wang, Y. Han, J. Zhu, W. Hieringer, J. Kuttner, G. Hilt, J. M. Gottfried, *Angew. Chem. Int. Ed.* **2013**, *52*, 4668; *Angew. Chem.* **2013**, *125*, 4766.
[12] L. Lafferentz, V. Eberhardt, C. Dri, C. Africh, G. Comelli, F. Esch, S. Hecht, L. Grill, *Nat. Chem.* **2012**, *4*, 215.
[13] L. Grill, M. Dyer, L. Lafferentz, M. Persson, M. V. Peters, S. Hecht, *Nat. Nanotechnol.* **2007**, *2*, 687.
[14] A. Saywell, J. Schwarz, S. Hecht, L. Grill, *Angew. Chem. Int. Ed.* **2012**, *51*, 5096; *Angew. Chem.* **2012**, *124*, 5186.
[15] L. Lafferentz, F. Ample, H. Yu, S. Hecht, C. Joachim, L. Grill, *Science* **2009**, *323*, 1193.

 © 2016 Wiley-VCH Verlag GmbH & Co. KGaA, Weinheim

[16] J. A. Lipton-Duffin, O. Ivasenko, D. F. Perepichka, F. Rosei, *Small* **2009**, *5*, 592.
[17] J. Cai, P. Ruffieux, R. Jaafar, M. Bieri, T. Braun, S. Blankenburg, M. Muoth, A. P. Seitsonen, M. Saleh, X. Feng, K. Müllen, R. Fasel, *Nature* **2010**, *466*, 470.
[18] S. Linden, D. Zhong, A. Timmer, N. Aghdassi, J. H. Franke, H. Zhang, X. Feng, K. Müllen, H. Fuchs, L. Chi, H. Zacharias, *Phys. Rev. Lett.* **2012**, *108*, 216801.
[19] D. Zhong, J.-H. Franke, S. K. Podiyanachari, T. Blömker, H. Zhang, G. Kehr, G. Erker, H. Fuchs, L. Chi, *Science* **2011**, *334*, 213.
[20] S. Boz, M. Stöhr, U. Soydaner, M. Mayor, *Angew. Chem. Int. Ed.* **2009**, *48*, 3179; *Angew. Chem.* **2009**, *121*, 3225.
[21] M. In't Veld, P. Iavicoli, S. Haq, D. B. Amabilino, R. Raval, *Chem. Commun.* **2008**, 1536.
[22] M. Abel, S. Clair, O. Ourdjini, M. Mossoyan, L. Porte, *J. Am. Chem. Soc.* **2011**, *133*, 1203.
[23] R. Gutzler, H. Walch, G. Eder, S. Kloft, W. M. Heckl, M. Lackinger, *Chem. Commun.* **2009**, 4456.
[24] J. F. Dienstmaier, A. Gigler, A. J. Goetz, P. Knochel, T. Bein, A. Lyapin, S. Reichlmaier, W. M. Heckl, M. Lackinger, *ACS Nano* **2011**, *5*, 9737.
[25] M. Bieri, M. Treier, J. Cai, K. Ait-Mansour, P. Ruffieux, O. Gröning, P. Gröning, M. Kastler, R. Rieger, X. Feng, K. Müllen, R. Fasel, *Chem. Commun.* **2009**, 6919.
[26] S. Ami, C. Joachim, *Phys. Rev. B* **2002**, *65*, 155419.
[27] J. Adisoejoso, T. Lin, X. S. Shang, K. J. Shi, A. Gupta, P. N. Liu, N. Lin, *Chem. Eur. J.* **2014**, *20*, 4111.
[28] P. Ruffieux, O. Gröning, M. Bielmann, C. Simpson, K. Müllen, L. Schlapbach, P. Gröning, *Phys. Rev. B* **2002**, *66*, 073409.
[29] M. Koch, F. Ample, C. Joachim, L. Grill, *Nat. Nanotechnol.* **2012**, *7*, 713.
[30] G. Meyer, J. Repp, S. Zöphel, K.-F. Braun, S. W. Hla, S. Fölsch, L. Bartels, F. Moresco, K.-H. Rieder, *Single Mol.* **2000**, *1*, 79.
[31] C. Nacci, F. Ample, D. Bleger, S. Hecht, C. Joachim, L. Grill, *Nat. Commun.* **2015**, *6*, 7397.

Received: June 3, 2016
Revised: August 1, 2016
Published online: September 16, 2016

 © 2016 Wiley-VCH Verlag GmbH & Co. KGaA, Weinheim